Author's Accepted Manuscript

Portable optical aptasensor for rapid detection of mycotoxin with a reversible ligand-grafted biosensing surface

Lan-hua Liu, Xiao-hong Zhou, Han-chang Shi

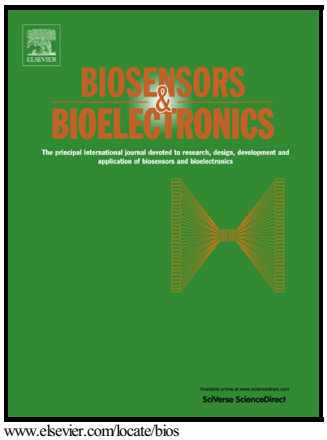

www.elsevier.com/locate/bios

PII: S0956-5663(15)30129-9
DOI: http://dx.doi.org/10.1016/j.bios.2015.05.033
Reference: BIOS7695

To appear in: *Biosensors and Bioelectronic*

Received date: 26 March 2015
Revised date: 11 May 2015
Accepted date: 12 May 2015

Cite this article as: Lan-hua Liu, Xiao-hong Zhou and Han-chang Shi, Portable optical aptasensor for rapid detection of mycotoxin with a reversible ligand-grafted biosensing surface, *Biosensors and Bioelectronic,* http://dx.doi.org/10.1016/j.bios.2015.05.033

This is a PDF file of an unedited manuscript that has been accepted for publication. As a service to our customers we are providing this early version of the manuscript. The manuscript will undergo copyediting, typesetting, and review of the resulting galley proof before it is published in its final citable form. Please note that during the production process errors may be discovered which could affect the content, and all legal disclaimers that apply to the journal pertain.

ACCEPTED MANUSCRIPT

Portable optical aptasensor for rapid detection of mycotoxin with a reversible ligand-grafted biosensing surface

Lan-hua Liu, Xiao-hong Zhou[1], Han-chang Shi

State Key Joint Laboratory of ESPC, School of Environment, Tsinghua University, Beijing 10084, China

Abstract: As food safety is gaining prominence as a global issue, the demand for developing rapid, simple, on-site, accurate and low-cost biosensor technologies will continue to grow. This study demonstrates an evanescent wave optical aptasensor with a reversible ligand-grafted biosensing surface for rapid, sensitive and highly selective detection of ochratoxin A (OTA) in food. In this system, the OTA molecules were covalently immobilized onto the surface of an optical fiber using glutaraldehyde and ethylenediamine as space linkers. An integrated evanescent wave all-fiber (EWA) biosensing platform was developed for investigating the binding kinetics between the tethered ligand and free OTA-aptamer, the performance of the aptamer-based bioassay and the reversibility of biosensing surface. The affinity constant (K_a) of aptamer with tethered OTA was measured to be 2.2×10^8 M^{-1} based on the EWA biosensing platform. With a competitive detection mode, the quantification of OTA over concentration ranges from 0.73 μg L^{-1} to 12.50 μg L^{-1} with a detection limit of 0.39 μg L^{-1}. The performance of the aptasensor with other interfering mycotoxins and spiked real wheat samples shows high specificity and selectivity, good recovery, precision, and accuracy, indicating that it can be applied for on-site, inexpensive and easy-to-use monitoring of OTA in real samples. Moreover, since the organic ligands are grafted onto the fiber surface, this strategy may avoid the potential disadvantages caused by immobilizing the nucleic acid biomolecules, such as weak restoration to the original DNA conformation after repeated uses.

Keywords: Aptasensor; Evanescent wave; Fluorescence; Ochratoxin A; Reversibility

1. Introduction

The worldwide contamination of foods and feeds with mycotoxins is a significant

[1] Email: xhzhou@mail.tsinghua.edu.cn
Tel: 8610-62796953; Fax: 8610-62771472

Accepted manuscript

issue due to their adverse effects on humans, animals, and crops that result in illnesses and economic losses (Hussein et al., 2001). Traditional quantification technologies of mycotoxins, such as high performance liquid chromatography, although accurate with low detection limits, require expensive instrumentation, intensive labor, sophiscated operations, as well as complicated sample preparation steps, which prohibit potential real-time and on-site practical applications. Therefore, the demand for rapid, simple, on-site, yet accurate and low-cost biosensor technology will continue to grow.

Aptamers, first reported in 1990, have attracted much attention and offered themselves to be ideal candidates as biocomponents in biosensors (aptasensors), possessing many advantages over state of the art affinity sensors, such as a broad range of target, chemical synthesis resulting in little or no batch to batch variation (O'Sullivan, 2002). Since then, numerous optical (Sassolas et al., 2011), electrochemical (Radi et al., 2006), and other aptamer-based sensors have been developed. Among them, the assay protocol of immobilizing DNA probe (e.g., aptamer, aptamer-complementary oligonucleotides) on a solid sensing surface were usually adopted (Han et al., 2010), making it critical and challengeable to keep the integration of nucleic acid surface during the regeneration and the restoration to its original DNA conformation after repeated uses (Wang et al., 2015). The change of original single-stranded DNA conformational, the activity loss of aptamer and the lost of probe molecules from the support surface after repeated uses are inevitable (Liu et al., 1999; Du et al., 2005). Although the regeneration of DNA biosensors could be achieved by either thermal or chemical methods, there are few platforms robust enough to be reused for more than 25 times (Radi et al., 2006). In addition, matrix complexity in real samples can produce interference or cross-reaction in the nucleic acid-based detection systems, which is regarded as another greatest challenge for the development of aptasensors (Torres-Chavolla et al., 2009).

To meet these challenges, we have developed a simple and robust aptamer-based evanescent wave optical all-fiber biosensor with a reversible ligand-grafted fiber for the rapid and sensitive detection of mycotoxins in real samples. Ochratoxin A (OTA), one of the most dangerous mycotoxins found in food and beverages (Cruz-aguado et al., 2008), was selected as a model target. In this strategy, the ligand of OTA was

Accepted manuscript

covalently immobilized on an optical fiber surface by introducing the linker, which may avoid the potential disadvantages caused by the immobilization of nucleic acids, mainly regarding the deficiency in reliably reusable ability due to the abovementioned reasons. Moreover, the amplitude of the evanescent wave decreases exponentially and confines transducible optical signals within a discrete distance from the support surface (usually no more than one-half the wavelength of the excitation light), minimizing interference or contribution from components in the bulk phase (Taitt et al., 2005; Mukundan et al., 2009; Ligler et al., 2009), and thus the proposed biosensor is expected to be less susceptible to sample matrix effects. Based on the established evanescent wave all-fiber (EWA) biosensing platform, the binding kinetics between the immobilized ligand and free fluorescence labeled OTA aptamer, the performance of the aptamer-based bioassay and reversibility of the biosensing surface were fully evaluated.

2. Experiments

2.1 Reagents and materials

N-(3-dimethylaminopropyl)-N'-ethyl-carbodiimide hydrochloride (EDC), N-hydroxysuccinimide (NHS), N,N-Dimethylformamide (DMF), ethylenediamine, 3-aminopropyltriethoxysilane (APTS), glutaraldehyde (GA), bovine serum albumin (BSA), Ochratoxin A (OTA), Aflatoxin B1 (AFT B1), Deoxynivalenol (DON) were purchased from Sigma-Aldrich (USA). Other chemicals were purchased from Sinopharm Chemical Reagent Co. Ltd (China). All chemicals were analytical grade if not specified and used directly without further purification.

The following oligonucleotides were synthesized from Takara Biotechnoly Co. Ltd (China).

Fluorescent dye labeled OTA-aptamer:

5′-GAT CGG GTG TGG GTG GCG TAA AGG GAG CAT CGG ACA-Cy5.5-3′

Twenty consecutive T-bases single-stranded DNA (T-20) for blocking the potential non-specific sites on the fiber surface:

5′-TTT TTT TTT TTT TTT TTT TT-3′

Accepted manuscript

ACCEPTED MANUSCRIPT

Buffers used in this work:

Binding buffer: 10 mM Tris, 120 mM NaCl and 10 mM $CaCl_2$, pH 8.5

Wash buffer: 0.5% SDS, pH 1.9

All buffers were prepared by DI water (18.2 MΩ cm).

2.2 Apparatus

Figure 1A presents the schematic of EWA biosensing platform which has been proposed as our previous described (Wang et al., 2015). Briefly speaking, a 635 nm, 10 mW pulse diode laser with a pigtail was coupled into a multi-mode fiber probe through an optical fiber bundle. Due to the total internal reflection of incident light in the fiber transducer, the evanescent wave was generated on the surface and interacted with surface-captured fluorophores, thus inducing fluorescence excitation. After that, the emitted fluorescence collected by the fiber probe was passed through the same optical fiber bundle, and subsequently filtered by means of a bandpass filter and detected by photodiodes through lock-in detection. The probe fiber was embedded in a glass flow cell with size of 55 mm in length and 2 mm in diameter. All reagents were pumped by a flow delivery system using a peristaltic pump. The controls of fluid delivery system and data acquisition and processing were automatically performed by a built-in computer.

2.3 Chemical modification of the fiber probe

The combination tapered fiber probe with maximum fluorescence collection capacity was produced by the tube-etching method as described previously by our research group (Long et al., 2008). As shown in Fig. 1B, the bare fiber was firstly introduced with hydroxyl groups, and then coated with a reactive silane layer by adding amino-terminal silanes (APTS). The functionalized amino groups on the fiber were allowed to react with GA and ethylenediamine, which acted as the linkers to conjugate OTA molecules through the traditional EDC/sulfo-NHS chemistry. The linkers serves as both suitable and biologically compatible spacers between the amino-modified fiber and OTA molecules, also in an attempt to reduce the steric hindrances for binding affinity interaction between the immobilized OTA and the free

Accepted manuscript

OTA-aptamer sequences. Finally, the fiber was treated with 2 mg ml^{-1} BSA for 1 h to block the non-specific binding sites and stored at 4 ˚C before use.

A detailed description of the experimental procedures can be found in the supplementary experimental procedures (see Supplementary Materials, Fig. S1).

2.4 Sensing mechanism for OTA detection

A competitive detection mode was adopted. Samples containing different concentrations of OTA were pre-incubated with a given concentration of fluorescence-labeled OTA-binding aptamer, and then detected by the EWA biosensing platform. A higher concentration of OTA led to less fluorescence-labeled aptamer binding to the fiber surface, and thus a lower fluorescence signal.

Figure 1B illustrated the competitive affinity assay of the aptamer-based evanescent wave optical biosensor for detection of OTA. During one test assay, 200 nM T-20 was firstly introduced into the flow cell to block the potential non-specific sites for DNA probe on the modified fiber surface. And then different concentrations of 200 μL OTA solutions was mixed with a predefined concentration of 200 μL Cy5.5-labeled OTA-aptamer for a certain constant pre-incubation time and pumped into the flow cell at a constant flow rate of 2 mL min^{-1} for 10 s and then reacted for another 2 min. During the reaction, the free OTA in solution and the ligand immobilized onto the fiber surface simultaneously and competitively bound with the fluorescence-labeled aptamers. Once the equilibrium state of this competitive affinity interaction was reached, the peak value of fluorescence intensity was recorded and inversely proportional to the OTA concentration in the samples. Finally, a regeneration process was performed by rinsing the fiber probe with SDS solution (0.5%, pH 1.9) at a constant flow rate of 2 mL min^{-1} for 50 s and washed with binding buffer for another 50 s, leaving it ready for a new test cycle.

3. Result and discussion

3.1 Binding kinetics

Figure 1C shows the typical fluorescence time trace during a complete assay cycle, which displayed the dynamic process of the biological affinity interaction between the

Accepted manuscript

immobilized OTA and the 2 nM Cy5.5-labeled OTA-aptamer sequences both in the absence and presence of 5 μg L^{-1} OTA in test samples. Regarding a real-time signal profile, the fluorescence intensity was increased as the aptamer bound to the fiber surface over time, expected to the peak value as the full binding equilibrium reached, and decreased due to introducing 0.5% SDS and binding buffer to treat the fiber successively. As we expected, the presence of OTA in the samples resulted in significantly decreased fluorescence intensity, which should be reversely proportional to the OTA concentration.

Knowledge on binding kinetics at a solid-phase interface is critical for the design and optimization of aptamer-based biosensor technologies (De-los-Santos-Álvarez et al., 2009; Long et al., 2011; Prabhakar et al., 2011; Castillo et al., 2012; Wu et al., 2012). In addition to serving as a transduction technique in analytical devices, the established evanescent wave fiber biosensing platform has the potential to provide detailed information about the affinity and kinetics of biomolecular interactions with high sensitivity (Long et al., 2011). Fig. 1D shows the kinetics of the association between surface-tethered OTA and 2 nM Cy5.5-labeled OTA-aptamer in solution and dissociation of the bound aptamer in the presence of 1 μM OTA in solution. To measure the affinity kinetic parameters of free aptamer with the immobilized ligand, the resulting fluorescence signals were analyzed theoretically and seems fitted to a first-order exponential growth during the association phase and a first-order exponential decay during the dissociation phase as similar as proposed by other studies (De-los-Santos-Álvarez et al., 2009; Long et al., 2011), see the green and red curve-fitting lines in Fig. 1D).

Association phase:

$$I(t) = A(1 - e^{-(k_s[apt] + k_d)t})$$

Dissociation phase:

$$I(t) = Be^{-k_d t} + C$$

Where I(t) was the observed fluorescence intensity at time, [apt] was the used aptamer concentration, k_s was the associated binding rate constant, k_d was the dissociated

Accepted manuscript

binding rate, A, B and C were constants. $K_a=k_s/k_d$ was the equilibrium association constant. i.e. the affinity constant. Our simulation results showed that the associating binding rate of $k_s[apt]+k_d$ was obtained to be 0.013 s^{-1}, which was in agreement with previous data measured by the commercial SPR instrument, such as 0.0156 s^{-1} for neomycin B and its aptamer (De-los-Santos-Álvarez et al., 2009). Although immobilization of ligand may introduce mass transport effects due to the lower diffusion coefficient of the large biomolecules (De-los-Santos-Álvarez et al., 2009), full equilibrium is however not mandatory for quantification, and hence, adopting the ligand-grafted solid stage biosensing strategy will not influence the speed-up of the assay. As shown in Fig. 1C, the whole time for one assay was no more than 10 min even if the pre-incubation time was considered. Moreover, k_d was simulated to be 0.009 s^{-1} according to the profile of dissociation phase. Therefore, k_s =2×10^6 $M^{-1}s^{-1}$ was obtained, resulting in the equilibrium association constant of K_a to be 2.2×10^8 M^{-1}. The affinity constant was one or two orders of magnitude larger than the homogenous assays, such as 5×10^6 M^{-1} (Cruz-aguado et al., 2008) obtained from the equilibrium dialysis; and comparable with the heterogeneous assays through immobilization of aptamer probes, such as 1.21×10^7 M^{-1} (Prabhakar et al., 2011), 1.21×10^8 M^{-1} (Castillo et al., 2012) and 7.5×10^{10} M^{-1} (Wu et al., 2012) obtained from electrochemical impedance spectroscopy. The very low K_a value, as a measure of the affinity between the free nucleic acid biomolecules to the tethered ligand on the fiber surface, indicates the high stability of the ligand-nucleic acid complex, which maybe attribute to the scientific design of the linkers between the fiber surface and the ligand and be beneficial to the sensitivity improvement of this method. Moreover, it also validated that the simple biosensing platform presented here could provide an alternative technique in characterizing DNA/DNA hybridization and small molecule-nucleic acid interactions for many applications.

3.2 Optimization of aptamer-based bioassay

Optimization processes were conducted to identify the optimal sensing conditions on the evanescent wave aptasensor for OTA detection. Three key factors for the

Accepted manuscript

competitive bioassay as suggested by the previous studies (Baldrich et al., 2004; Cruz-aguado et al., 2008; Wu et al., 2012), including the Cy5.5-labeled OTA-aptamer concentration, the pre-incubation time and the calcium concentrations in ligand-aptamer binding buffer were investigated.

Different pre-incubation times (1, 3, 5, 10 and 15 min) for the Cy5.5-labeled OTA-aptamer and samples were investigated as shown in Fig. S2A (1 μg L^{-1} OTA and 2 nM Cy5.5-labeled OTA-aptamer used). It is expected that a longer incubation time would yield a more stable OTA-aptamer complex, contributing to a more stable fluorescence signal. The fluorescence signal was recorded along with the variable pre-incubation times. We observed that the fluorescence signals decreased with the increased pre-incubation times and 5 min was enough for binding the stale complex between the OTA and the OTA-aptamer, and therefore 5 min of pre-incubation time was chosen for all the subsequent analysis. The relationship of the different Cy5.5-labeled aptamer concentrations (0.1, 0.5, 1, 2 and 5 nM) versus the fluorescence signals were investigated and the depicted curve accorded with the logistic model with a common "S" shape (Fig. S2B). The point of inflection for the "S" shape profile occurred at 1 nM Cy5.5-labeled aptamer, indicating that the highest sensitivity caused by the change in aptamer concentration can be reached, therefore, 1 nM Cy5.5-labeled aptamer was applied in the following experiments. The presence of divalent cations, Ca^{2+} or Mg^{2+}, is essential for the specific recognition of OTA by the OTA-aptamer (Cruz-aguado et al., 2008). Fig. S2C shows the EWI signals responding to 1nM OTA-aptamer in binding buffer with different Ca^{2+} concentrations. The optimum Ca^{2+} concentration in binding buffer used for the OTA detection was 10 mM.

3.3 Detection performance

Sensitivity and detection limit

Based on the optimized assay conditions, the temporal fluorescence responses for different concentrations of OTA in a test cycle were recorded in Fig. 2A. An observable decrease of the fluorescence response to OTA was observed by adding

Accepted manuscript

OTA to the OTA-aptamer. When the OTA concentration was increased to 400 μg L^{-1}, a slight fluorescence signal was observed, indicating that non-specific adsorption on the fiber surface was negligible due to treating both BSA and T-20 as the shielding agents. Fig. 2B shows the calibration curve of OTA, which was normalized by expressing the signal decreases of each standard point as the ratio to that of the blank sample containing no OTA. The symmetric dose-response data was fitted with a four-parameter logistic model (see Supplementary Materials S3 and Fig. S3 for more details) because the model was confirmed with reliable accuracy and recommended for curve fitting in such ligand binding assays (Little, 2004; Findlay et al., 2007). Actually, the four-parameter logistic model has been widely adopted for ligand binding assays in the previously reported studies, such as the immunoassay (Baldrich et al., 2004; Long et al., 2008) and the aptamer-based affinity assay (Wang et al., 2015). The working range for OTA detection was from 0.73-12.50 μg L^{-1} with a detection limit of 0.39 μg L^{-1}, which was lower than the maximum limits for OTA residue in food and feeds executed by the European Union (European Commission, 2006), such as 5 μg kg^{-1} for raw cereal grains and 3 μg kg^{-1} for all cereal-derived products. The sensitivity and detection limit of the proposed aptasensor were also comparable with the reported results obtained by other methods (See Table S1, Supplementary Materials). We attributed the high sensitivity of the developed method to its binding style through using the tethered ligand of OTA as the recognition element of biosensing. It might maximize the binding efficiency between the aptamer and its target of interest because it was similar to the process of identifying the OTA-aptamer as described by Cruz-aguado et al. (2008). In their work, OTA was immobilized on an agarose-based resin and used for binding DNA sequences with high affinity and specificity to OTA.

Selectivity

The cross-reactivity of this method for OTA detection was estimated by analyzing the binding curves for OTA, AFT B1 and DON over the 0.001 to 400 μg L^{-1} concentration range as shown in Fig. 2C. Comparing the IC_{50} values for the target and the

Accepted manuscript

cross-reacting compounds potentially present in the sample is a typical method to estimate the cross-reactivity of a technique (Franek et al., 1999). The IC_{50} values were calculated to be 3.01 μg L^{-1}, >10 000 μg L^{-1}, and >10 000 μg L^{-1} for OTA, AFT B1 and DON, respectively. These data corresponded to the cross-reactivity values of 100% for OTA, <0.01% for AFT B1, and <0.01% for DON, indicating that the selectivity of the aptamer-based optical biosensor is convincing even used in a complicated matrix containing other mycotoxins.

Reusability

Reusability of a biosensor is a desired and attractive feature for its application and has received considerable attention, and it is closely related with the effective reversibility of biosensing surface. In the assay herein described, OTA was grafted on the fiber surface by using the covalent coupling approach as mentioned above. The biosensing fiber surface can be reversible using 0.5% SDS solution, pH 1.9 without damage of its biosensing properties. Fig. 2D shows the good measurement-to-measurement reproducibility and reversibility of the proposed aptasensor for hundreds cycles of measurements during five weeks. Due to the convincing merits of ligand-grafted biosensing surface, such as more robust for harsh regeneration conditions, and less susceptible to the biological contaminants inevitable during the long-time use for the real samples, one fiber was reused for more than hundreds cycles of measurements without any significant loss in performance during two-month testing period for this study. The fiber surface was investigated by using X-ray photoelectron spectrum (XPS). XPS is capable of not only providing information about the chemical bonding on the surface but also the semi-quantitative analysis giving the rough atomic concentration of interest (Zhang et al., 2002). The Cl 2p spectra of bare fiber, modified fiber before and after use were showed in Fig. 3. There is no Cl 2p peak at 197.94 eV for bare fiber, and as expected, obvious Cl 2p peaks observed for modified fibers, indicating that the OTA molecule was successfully modified on the fiber surface. The areas of the Cl 2p peak at 197.94 eV were estimated and used for quantification of Cl atoms residual functionalized on the fiber probe surface. The

Accepted manuscript

results show that about 76% of Cl atoms still existed even after about 200 times of measurements, indicating the robust and stable ligand-grafted biosensing surface was achieved.

Recoveries of wheat samples

The matrix susceptibility caused by component variability in several environmental water samples is a source of potential interference and should thus be considered to verify the accuracy and applicability of the ligand-grafted EWA aptasensor. In the present study, the percentage recovery (%) of three wheat powder samples was estimated by spiking with three level concentrations of standard OTA (Table S2, 2.0 μg L^{-1}, 5.0 μg L^{-1} and 10.0 μg L^{-1}). All samples were measured before spiking to ensure no contamination of OTA. The percent recoveries of the OTA added to the wheat samples at different concentrations ranged from 89% to 106%. All coefficients of variation were acceptable and did not exceed 16% (n=3). These results confirm that the proposed aptamer-based EWA optical biosensor with a reversible ligand-grafted biosensing surface is robust and considerably resistant to the environmental matrix and thus applicable to the OTA detection in real samples.

4. Conclusion

A portable optical aptasensor for rapid detection of mycotoxin was successfully achieved by the effective integration of an evanescent wave all-fiber biosensing platform with an aptamer-based competitive bioassay. Compared with traditional techniques, this system provides several prominent advantages. First, using the evanescent wave fiber as the transducer enable the fluorescence bioassay process to confine the transducible optical signals to within a narrow distance from the support surface, therefore, minimizing interference or contribution from components in the bulk phase, and thus was less susceptible to sample matrix effects. Second, the ligands, instead of nucleic acid sequences in the traditional aptasensors, were grafted on the fiber surface as the recognition element, which enabled the functional fiber reversible, stable, robust for harsh regeneration conditions, less susceptible to the biological contaminants and easy to store. Third, the linkers of ethylenediamine-modified

Accepted manuscript

ACCEPTED MANUSCRIPT

glutaraldehyde was introduced as spacers between the fiber and the OTA molecules to prevent steric hindrance and maintain the high activity of the functionalized fiber probe for its receptor. Finally, base on the competitive immunoassay mode, the biosensing assay of OTA using the proposed EWA biosensing platform was featured good characteristics with its high sensitivity, selectivity, rapidity, and ease of use.

Acknowledgements

This research is supported by the Major Scientific Equipment Development Project of China (2012YQ030111) and Beijing Nova Program (Z141109001814078).

References

Baldrich E., Restrepo A., O'sullivan C.K., 2004. Analytical Chemistry 76, 7053-7063.

Castillo G., Lamberti I., Mosiello L., Hianik T., 2012. Electroanalysis 24, 512-520.

Cruz-aguado J.A., Penner G., 2008. Journal of Agricultural and Food Chemistry 56, 10456-10461.

De-los-Santos-Álvarez N., Lobo-Castañón M.J., Miranda-Ordieres A.J., Tuñón-Blanco P., 2009. Biosensors and Bioelectronics 24, 2547-2553.

Du H, Strohsahl C.M., Camera J., Miller B.L., Krauss T.D., 2005. Journal of the American Chemical Society 127, 7932-7940.

European Commission, 2006. Commission Regulation No. 1881/2006: Commission Regulation (EC) No. 1881/2006 of 19. Official Journal of the European Union L, 364, 5-24.

Findlay J.W.A., Dillard R.F., 2007. The AAPS Journal, 9(2), E260-E267.

Franek M, Kolar V, Deng A.P., Crooks S., 1999. Food &Agricultural Immunology 11, 339-349.

Han K., Liang Z.Q., Zhou N.D., 2010. Sensors 10, 4541-4557.

Hussein H.S., Brasel J.M., 2001. Toxicology 167, 101-134.

Ligler F.S., 2009. Analytical Chemistry 81, 519-526.

Little J.A., 2004. Chromatographia 59, S177-181.

Liu X.J., Tan W.H.,1999. Analytical Chemistry 71, 5054-5059.

Long F., He M., Shi H.C., Zhu A.N., 2008. Biosensor and Bioelectronics 23, 952-958.

Accepted manuscript

ACCEPTED MANUSCRIPT

Long F., Wu S.X., He M., Tong T.Z., Shi H.C., 2011. Biosensor and Bioelectronics 26, 2390-2395.

Mukundan H., Anderson A.S., Grace W.K., Grace K.M., Hartman N., Martinez J.S., Swanson B.I., 2009. Sensors 9, 5783-5809.

O'Sullivan C.K., 2002. Analytical and Bioanalytical Chemistry 372, 44-48.

Prabhakar N., Matharu Z., Malhotra B.D., 2011. Biosensors and Bioelectronics 26, 4006-4011.

Radi A.E., Sanchez J.L.A., Baldrich E., O'Sullivan C.K., 2006. Journal of the American Chemical Society 128, 117-124.

Sassolas A., Blum L.J., Bouvier B.D.L., 2011. Biosensor and Bioelectronics 26, 3725-3736.

Taitt, C.R., Anderson, G.P., Ligler F.S., 2005. Biosensors and Bioelectronics 20, 2470-2487.

Torres-Chavolla E., Alocilja E.C., 2009. Biosensor and Bioelectronics 24, 3175-3182.

Wang R.Y., Xiang Y., Zhou X.H., Liu L.H., Shi H.C., 2015. Biosensor and Bioelectronics 66, 11-18.

Wu J., Chu H., Mei Z., Deng Y., Xue F., Zheng L., Chen W., 2012. Analytica Chimica Acta 753, 27-31.

Zhang N., Xie J., Varadan V.K., 2002. Smart Materials and Structures 11, 962-965.

Accepted manuscript

ACCEPTED MANUSCRIPT

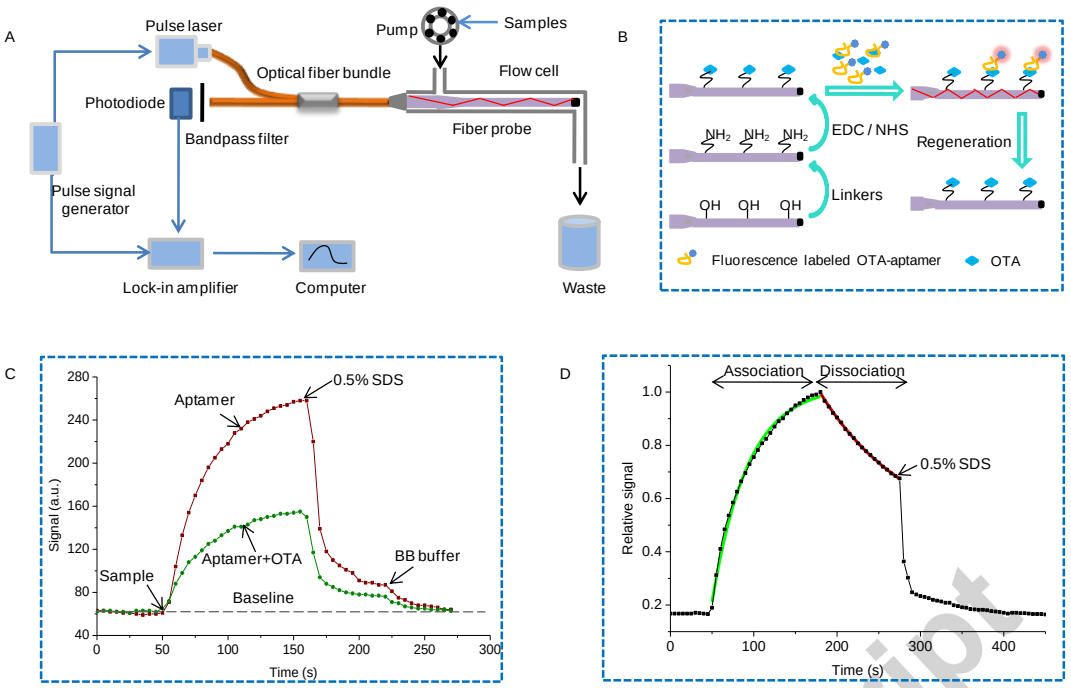

Fig. 1 (A) Schematic set-up of evanescent wave all-fiber optical biosensing platform (EWA); (B) Preparation of ligand-grafted biosensor by conjugating carboxyl of OTA to amine-coated fiber through the EDC/NHS chemistry and the corresponding competitive sensing mechanism for OTA detection; (C) Representative signal profiles for binding 1 nM aptamer without OTA (dark red dotted line) and with 5 μg L^{-1} OTA (green dotted line) by EWA; (D) Kinetics of the association between surface-tethered OTA and 2 nM Cy5.5-labeled OTA-aptamer in solution and dissociation of the bound aptamer in the presence of 1 μM OTA in solution, expressed as the relative fluorescence signals with time, and the corresponding binding kinetics assays for the OTA-nucleic acid interactions on the EWA platform (marked by the green and red lines)

Accepted manuscript

ACCEPTED MANUSCRIPT

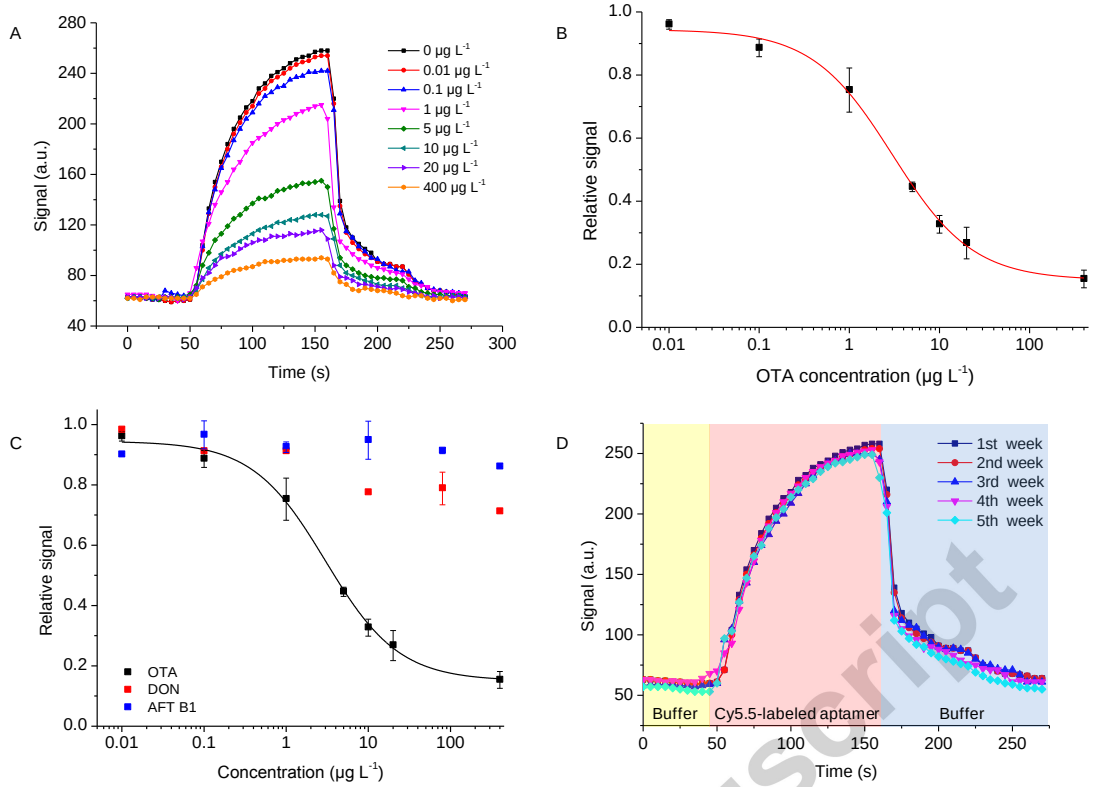

Fig. 2 (A) Temporal fluorescence responses for different concentrations of OTA (2 nM Cy5.5-labeled aptamer used); (B) Logarithmic calibration curve for OTA detection by using the proposed EWA optical aptasensor; (C) Competitive curves for OTA, DON and AET B1 obtained by using the OTA aptasensor; (D) Reversible real-time EWA signals for the ligand-grafted aptasensor experiencing hundreds cycles of measurements during five weeks (2 nM Cy5.5-labeled aptamer used)

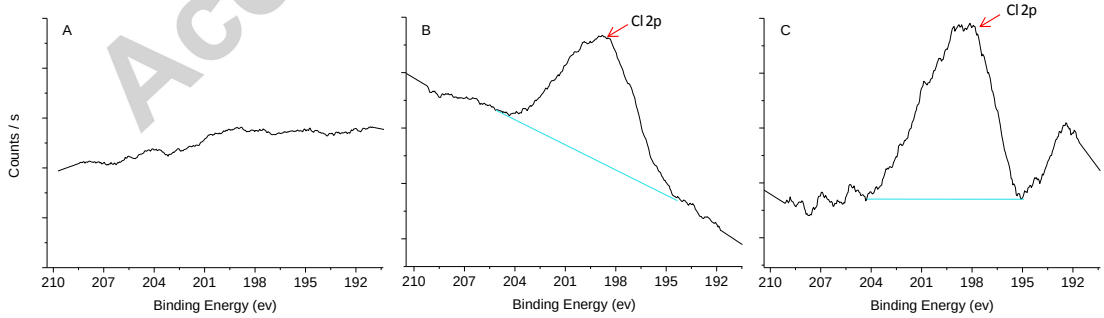

Fig. 3 Cl 2p XPS spectra of the fiber surface (A) before and (B) after the covalent immobilization with OTA and (C) used for hundreds of times

Highlights

Accepted manuscript

Portable optical aptasensor for rapid detection of mycotoxin was developed with a reversible ligand-grafted biosensing surface

The evanescent wave all-fiber (EWA) biosensing platform is an alternative technique for study of affinity interactions

Using the tethered ligand as the recognition element enable the aptasensor with reliably reusable ability

The EWA aptasensor was featured with sensitivity, specificity and accuracy for OTA detection in real samples

Accepted manuscript